On the Development of Interspecies Traumatic Brain Injury Correspondence Rules

Robert Saunders; X. Gary Tan; Amit Bagchi

ABSTRACT Traumatic brain injury analysis in human is exceedingly difficult due to the methods in which data can be collected, thus many researchers commonly implement animal surrogates. However, use of these surrogates is costly and restricted by ethical concerns and test logistics. Computational models and simulations do not have these constraints and can produce significant amounts of data in relatively short periods. This paper shows the development of a human head and neck model and a full body porcine model. Both models are developed from high-resolution CT and MRI scans and the latest low-to-high strain rate mechanical data available in the literature to represent tissue component material behaviors. Both models are validated against experiments from the literature and used to complete an initial interspecies correspondence rule development study for blast overpressure effects. The results indicate the similarities in the way injury develops in the pig brain and human brain but these similarities occur at very different insult levels. These results are extended by a study, which shows that blast peak pressure is the driving factor in injury prediction and, depending on the injury metric used, significantly different injuries could be predicted.

INTRODUCTION

Blast events accounted for nearly 70% of injuries in wounded service members, and are the main cause of traumatic brain injury (TBI).[1] Analysis of blast-induced TBI in humans is very difficult since the majority of collected data is from combat theaters without controlled insults or postmortem human subject (PMHS) testing, which may not represent the *in-vivo* human well.[2] Other researchers have used animals as human surrogates to obtain blast response data from the brain but such tests are often restricted. A number of animal species have been compared to humans for TBI response, but no one animal has shown to be superior to all others.[3,4] Rats are commonly used as surrogates for humans but due to their lissencephalic nature and dissimilar mass compared to the human, many researchers cast doubt about the applicability of the data for human injury.[5] Porcine subjects are much closer to the mass of an adult human, gyrencephalic, and believed to exhibit TBI responses similar to that of the human brain. As a way to establish interspecies TBI correspondence rules, this work will relate TBI in the pig with that in the human using computational simulation.

A number of models of varying fidelity have been generated over the past decades, involving segmentation of medical imaging data and calibration and implementation of complex constitutive models.[6–13] With the use of high-performance computing facilities, high-fidelity experimentally validated computational models with high strain rate biological material data can provide insight into TBI far beyond any experiment with relatively high accuracy. This paper develops a framework for comparing a computational human brain response with that of a computational porcine brain due to blast overpressure loading. The human head and porcine models are constructed from high-resolution medical imaging scans, which are digitally segmented then transformed into a finite element (FE) mesh. Latest low-to-high strain rate data available in the literature have been used to define tissue constitutive behaviors. The human brain model is validated against available PMHS experimental data for blunt impact, and the porcine model is validated against available experimental data for blast events. To develop a framework for correspondence rules, both human and porcine computational models are subjected to identical blast waves. The resulting brain injury assessment is predicted based on biomechanical measures and injury thresholds, such as pressure, shear stress, and shear strain, from the literature. The peak overpressure, positive phase duration, and orientation of blast are also varied in the human model to determine their effects on injury.

METHODS

The computational models in this work are based on (a) a 25-year-old Caucasian male representing a 50th percentile U.S. male, 1.8 m tall and weighing 81 kg; and (b) a 6-month-old male Yucatan pig with a weight of 30 kg.[14] The human model in this work consists of only a head and neck while the pig model of a full body.

Model Generation

Both the pig and human head models were generated from *in-vivo* magnetic resonance imaging (MRI) using semi-automatic segmentation in ScanIP software by Simpleware, Inc. (Synopsys, Mountain View, USA). The human scans

Multifunctional Materials Branch, Materials Science and Technology Division, U.S. Naval Research Laboratory, 4555 Overlook Ave. SW., Washington, DC 20375.

The views expressed in this paper are those of the authors and do not necessarily represent the official position or policy of the U.S. Government, the Department of Defense, or the Department of the Navy.

doi: 10.1093/milmed/usy360

were performed with a 1 mm isotropic resolution and the pig scans used a 0.8 mm isotropic resolution. These high-resolution scans allowed placing the necessary emphasis on details in the head and brain. For the human model, the MRI scans were supplemented by CAD representations of the other components such as the face and neck musculature.[15,16] The pig MRI scans were supplemented with 0.6 × 0.6 × 1.0 mm^3 resolution computed tomography (CT) scans to image and segment the pig torso. All major components of the human head and neck, and the pig head and body were included in the models shown in Figures 1 and 2 and listed in the first column of Table I.

Segmentation of the models produced surface representations of the human and pig model components, which are converted to a FE mesh using a multi-part surface decimation algorithm followed by a mixed Delaunay Advancing Front approach.[17] Thin membranous regions, such as the dura mater, are represented by shell elements while the remainder of the models is represented by solid tetrahedral elements. A tetrahedral mesh was chosen for its ability to best capture the complex geometric features in human and pig brains.[16] Quadratic tetrahedral elements are used for the nearly incompressible regions, such as the brain and CSF, to prevent volumetric locking exhibited by linear tetrahedral elements in

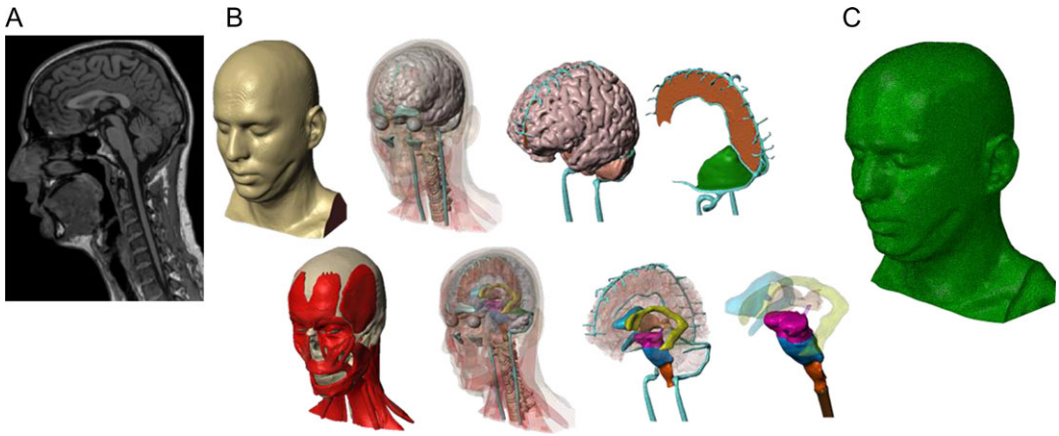

FIGURE 1. (A) High-resolution MRI scan of 50% percentile Caucasian male used to generate human FE model, (B) Surface representations of human model components after segmentation, and (C) Human model as meshed for implementation in an FE solver.

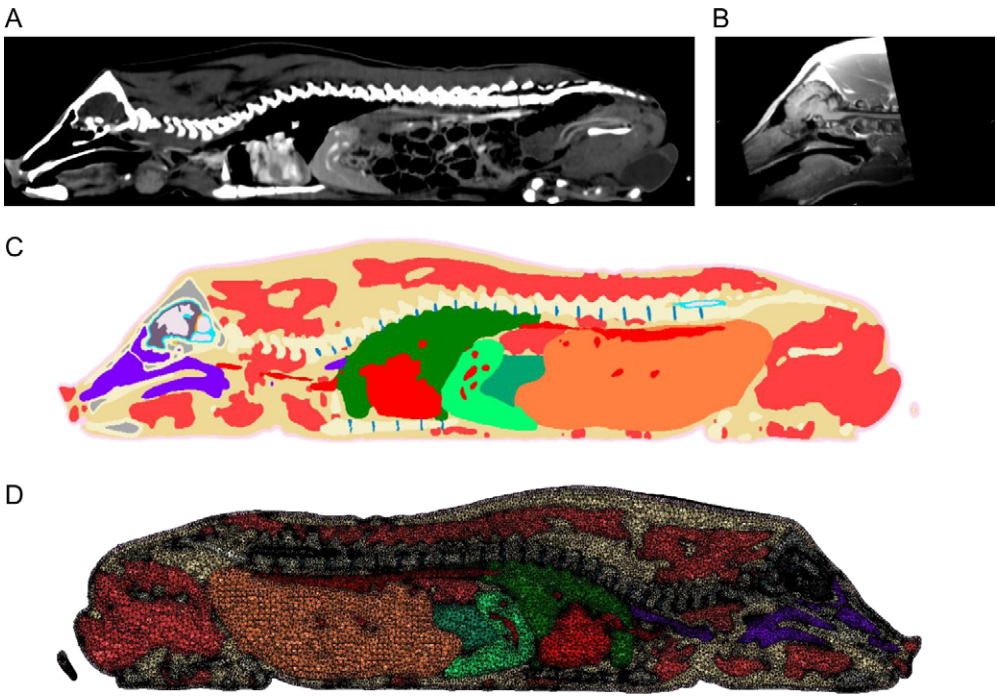

FIGURE 2. High resolution (A) full body CT and (B) head MRI scan of Yucatan pig used to generate pig FE model, (C) Surface representations of pig model components after segmentation, and (D) Pig model as meshed for implementation in an FE solver.

TABLE I. Human and Pig Anatomical Structures Included in the FE Models and Their Corresponding Constitutive Model Functional Forms

Component	Constitutive Model Functional Form
Sinus – frontal	Equation of state (ideal gas law)
Sinus – maxillary	
Airway	
Cerebrospinal fluid (CSF)	Hyperelastic (neo-Hookean)
Ventricles – lateral	
Ventricles – third	
Ventricles – fourth	
Ventricles – aqueduct of sylvius	
Ventricles – foramen of monro	
Venous sinuses and bridging veins	
Eyes (vitreous)	Hyperelastic (neo-Hookean)
Venous sinus and bridging vein walls (shell section)	Anisotropic hyperelastic (Holzapfel)
Pia mater (shell section)	Hyperelastic (Ogden)
Dura mater (shell section)	Hyperelastic (Ogden)
Falx cerebri	Hyperelastic (Ogden)
Tentorium cerebella	Hyperelastic (Ogden)
Sclera/cornea (shell section)	Hyperelastic (Ogden)
Intervertebral disks	Hyperelastic (Mooney–Rivlin)
Costal cartilage	Hyperelastic (Ogden)
Skull – cortical	Transversely isotropic viscoelastic (Prony Series)
Skull – cancellous	Transversely isotropic viscoelastic (Prony Series)
Mandible	Transversely isotropic viscoelastic (Prony Series)
Vertebrae	Viscoelastic (Prony Series)
Ribs	Viscoelastic (Prony Series)
Sternum	Viscoelastic (Prony Series)
Cerebrum – gray matter	Hyper-viscoelastic (Ogden, Prony series)
Cerebellum – gray matter	
Cerebrum – white matter	Hyper-viscoelastic (Ogden, Prony series)
Cerebellum – white matter	
Brain Stem – medulla	
Brain Stem – midbrain	
Brain Stem – pons	
Spinal cord	
Optic nerves	
Skin	Hyperelastic (Ogden)
Heart	Hyper-viscoelastic (Ogden, Prony series)
Muscles	Hyperelastic (Ogden)
Soft tissue (adipose)	Hyperelastic (Ogden)

Note that not all components are present in both models and components that are in both models share the same constitutive model parameters. Grouped materials share the same constitutive model parameters due to similarities in the material.

some cases. The mesh density required in the models was determined by conducting a convergence study on thick sagittal slices of the human brain. The results of this study suggested that an average element critical length of ~1 mm was sufficient to capture a blast pressure wave transmission through the brain. While a complete mesh convergence study could have been desirable, the cost of mesh generation, model definition, and computational time for analysis of these models would make such a study prohibitively expensive. The total number of elements in each model was 4.6 million for the human and 10 million for the pig.

Constitutive Representation

To complement the high-fidelity geometric representation of the human and pig subjects in the models, constitutive models are chosen to best emulate the biological materials over a range of loading rates and deformation levels. Note that due to a lack of data in the literature, both the human and pig models utilize the same constitutive models. Some authors have suggested that mechanical difference in the tissues between species may be small and this assumption has been made in this study as well.[18] The physical behavior of biological materials under mechanical loading often requires nonlinear, rate-dependent constitutive formulations.[19] The process to obtain these constitutive formulations and their required parameters uses a significant amount of experimental data for each component in the model, which may not be available in the literature due to complexity of experimentation required. Additionally, biological tissues generally have a high degree of anisotropy and are non-homogenous; further complicating the experimental process.[20]

The first step towards the constitutive model calibration is to identify an appropriate constitutive model, whose functional form will be able to reproduce the experimental data available. The published literature on biological tissue either is in the form of experimental data for a given component or as a constitutive model calibrated with well-defined parameters. A calibrated constitutive model is preferred for model construction. If a calibrated constitutive model is outdated or unavailable, considerably more effort is required to obtain a "good" parameter set. Some available programs have the ability to calibrate many constitutive models to a single data set rapidly, but may not be able to capture the complex, coupled, rate-dependent hyperelastic behavior exhibited by biological tissues or they may not be available to the modeler. In these cases, a functional form can be developed from the strain energy to capture the material behavior and an optimization routine with appropriate constraints must be implemented. The constitutive models chosen for the human and pig models of this work are summarized in Table I with complete details given in Brewick et al.[19]

Model Simulation

Two FE solvers, each with strengths and weaknesses, are used to simulate the human and pig models. The first code is Abaqus/Explicit (Dassault Systèmes Simulia Corp., Providence, RI, USA). Abaqus is a commercial code that is robust and highly utilized FE code with a number of applications and functions. However, due to the size of the models in this work, the license usage on the US Department of Defense High Performance Computing (HPC) systems becomes prohibitive, and precludes complex analyses, such as fluid structure

interactions and advanced coupled Eulerian–Lagrangian (CEL) analyses. A second code, Computational Biology (CoBi), is a DoD open-source, multi-physics code developed in C++ and is not restricted by license usage, making it well suited to utilize the vast computational resources of HPC for the coupled CEL analyses.[21,22]

While two independent solvers may not be ideal, both codes have been shown to produce identical results when identical parameters (hourglass stiffness, bulk viscosity, mass scaling, *etc.*) are used. Additionally, for simple cases (*e.g.*, a plane wave with known pressure-time history on a model), Abaqus produces the same results as CoBi but in slightly less time, mainly because of the use of different programming languages between the codes. However, when considering complex cases (*e.g.*, the full pig model simulated using the CEL method), CoBi is able to scale up and utilize a significantly higher number of computer cores than Abaqus, thus producing results faster than Abaqus. For these reasons, it was deemed appropriate to utilize both solvers.

Upon completion of each simulation, a script was used to process the biomechanical results in the pig and human brains (limited to the cerebrum, cerebellum, and brain stem). This script used biomechanical predictors likely to cause TBI (Table II) from published literature, to determine if an element in the brain had undergone a certain threshold pressure, shear stress, or shear strain that would represent clinically a brain injury.[10,23–28] The accuracy and validity of these thresholds are not the scope of this paper, and these can be improved as improved criteria are developed. Furthermore, many of the biomechanical injury thresholds can be ignored for a given analysis because either they are not triggered or a variable is triggered with multiple suggested thresholds but it serves no benefit to present the lower threshold results as it is obvious that if a higher threshold is triggered the lower must have been triggered.

RESULTS AND DISCUSSION

To demonstrate that a computational model solves the underlying systems of equations correctly and that the expected physical result is produced, a validation is necessary.[29,30] In this work, the validation of both the human and pig models is first shown followed by two studies on development of a framework for correspondence rules which use the validated models.

Human Model Validation

Human models for prediction of TBI are commonly validated against four blunt impact experiments on cadavers by Nahum et al., Trosseille et al., Hardy et al., and Yoganandan et al.[31–35] Blast events occur in a much shorter period than blunt impacts, thus the applicability of a validation against blunt data for blast analysis can be questioned. Another possible concern is the use of a PMHS to represent *in-vivo* humans, as it is known that the postmortem state changes the mechanical behavior of tissues.[2] It has also been reported in the literature that PMHS with dissimilar age, gender, and weight can have varying mechanical responses.[36–38] Inadequate documentation in experimental details, such as insufficient instrumentation location definition, insult description, *etc.*, associated with each validation case are not discussed here and instead a summary of the validation results is presented (Figs 3–6).

As shown in the figures, the results from each experiment agree well with those from the computational human model. In the Nahum et al.[31] case, the largest discrepancy in the results is in occipital region. In this countercoup region, it is speculated that this difference could be attributed to either the boundary conditions applied to the neck or the contact condition applied to the brain-CSF-dura-skull complex. As can be seen in Figure 3, a CSF sliding contact condition (as opposed to a CSF tie condition in the other cases) does not allow the transmission of a tensile pressure due to the

TABLE II. Biomechanical Thresholds of TBI Suggested by Various Authors

Metric	Limit	Injury	Reference Source
Pressure (kPa)	173	Mild TBI	10
	235	Severe TBI	
	−100	50% probability of concussion (DDM[a])	23
Effective (von Mises) stress (kPa)	11	Severe TBI	24
	26	50% probability of mild DAI[b]	25
	33	50% severe DAI	
Shear (Tresca) stress (kPa)	7.8	50% probability of mild TBI	10
Maximum principal strain (%)	5	Moderate DAI	26
	15	50% probability of DAI (CSDM[c])	23
	18	DAI	27
	20	50% probability of mild TBI	10
	21	50% probability of mild DAI	28
	26	50% probability of mild DAI	
Effective (von Mises) strain (%)	25	50% probability of mild DAI	25
	35	50% probability of severe DAI	

[a]DDM, dilatational damage measure.
[b]DAI, diffuse axonal injury.
[c]CSDM, cumulative strain damage measure.

separation of the dura and CSF. Further, the boundary conditions at the neck do not have an effect until at a later time period in the analysis when inertia of the model begins to become more significant.

In Figure 4, the results of Trosseille et al[32] demonstrate similar agreements with computational results as for the Nahum et al[31] case. In this instance, a difference in results is seen in the parietal region, and is consistent with previous model validations that have validated a computational head model against this work.[39] Figure 5 shows the results of Hardy et al[33,34] and demonstrate accurate capture of the peak pressure but not subsequent pressures by the computational simulations. This is believed to be a result of boundary conditions as suggested in the Nahum et al. validation. Lastly, the Yoganandan et al[35] case (Fig. 6) shows a strong agreement between the experiment and simulation up to the point of skull fracture, which is not implemented in the computational model.

Pig Model Validation

Animal testing data for pigs are available in the literature for shock tube loading. These datasets have been used to validate the computational pig model.[40] Initial efforts to validate the pig model were accomplished using Abaqus/Explicit. However, due to the complex nature of the shock wave interaction with the pig in the shock tube, a more accurate interaction of the shock front with the pig was necessary, and so the CEL method implemented in CoBi was used.[41] To facilitate this advanced large-scale simulation of a full pig inside a shock tube, a hexahedral mesh was used in the Lagrangian pig model for compatibility with the model used in the Eulerian analysis.

The shock wave propagation in the shock tube is modeled using a novel sequential 1D, 2D, 3D Eulerian simulation strategy to generate the pressure-time history over the entire surface of the pig, which is then used as input for the Lagrangian analysis to generate the biomechanical measures in the pig for the validation. The results of the CEL analysis using the parameters described in the experimental procedure described by Zhu et al are shown in Figure 7, and the validation results are shown in Figure 8.[40] Figure 8A shows the Eulerian analysis validation from the pencil gauge inside the shock tube. The computational model adequately captures the pencil gauge pressure profile, except the second peak in the experimental data. It is speculated that this second peak is due to the positioning of the pig in the shock tube causing the pig head not aligning with a significant reflected front from the tube wall. The simulation and experimental intracranial pressure data are in excellent agreement except the secondary peak pressure, as for the pencil gauge pressure profile.

Interspecies Correspondence

In order to develop a framework of the interspecies correspondence between the pig and the human biomechanical models, both of these models have been subjected to the same blast loading profiles as plane waves with a known pressure-time history. The blast pressure-time profiles have been derived from earlier free-field explosion experiments. Both the pig and human models are oriented for frontal and side-on loading. The models were subjected to three peak overpressures of 255, 345, and 427 kPa as schematically represented in Figure 9. The results of the case study are shown in Figures 10–12.

At 255 kPa peak overpressure (Fig. 10), 4 of the 15 available injury metrics are shown, as only these 4 had non-zero volume percentage of brain injuries. Further, none of these four metrics showed more than 1% injured brain volume. Due to uncertainty in the model segmentation, discretization, constitutive model calibration, etc., it is assumed that injured volumes below the 1% threshold are more likely noise rather than an actual predicted injury. Thus, at such small predicted injured volumes, we assume an injury is unlikely and statistically insignificant.

At 345 kPa peak overpressure (Fig. 11), the overall results are similar to those for the 255 kPa case. However, now the 173 kPa pressure-based injury criterion seems to be significant for the human head but not for the pig model. These lower injured brain volumes for the pig are to be expected due to their relatively large skull thickness. The predicted volume of injured brain using the 7.8 kPa Tresca stress (*i.e.*, maximum shear stress) criterion increases from the frontal orientation to the side-on in the pig model but not in the human model. In the frontal and side-on orientation, the human neck has approximately the same ability to rotate the head. In the prone position, the side-on orientation allows movement of the pig head similar to that of the human head, but in the frontal orientation, the body prevents such a motion. This increase in shear stress in the brain may be due to due to these head-neck motion limitations.

At the peak overpressure of 427 kPa (Fig. 12), the volume of the injured brain is quite significant for both the human and pig models. Excessive element distortion caused by very soft shear and volumetric behavior in the fluid cavities (e.g., sinuses and CSF) in the pig model at this pressure resulted in a smaller overall simulation time. The simulation results for the frontal case show that the injury to the pig brain based on pressure-based injury criterion is more pronounced, and the volume of injured brain based on Tresca stress criterion appears also appears to increase.

Both the pig model and the human model exhibit markedly different responses at the different pressures, as can be seen in Figures 10–12. As the input peak overpressure goes up the volume of the injured brain (i.e., the region of the brain that meets or exceeds the stress or strain criterion) increases. At higher pressures, not only the 173kPa pressure-based criterion is met (see Fig. 12, for example), but also the 235kPa pressure-based criterion is met for a smaller volume of the brain. Using multiple criteria thus allows a quantification of the severity of the injury at the higher pressures. Similar trends can also be seen for the pig brain, albeit to a much lesser extent than those in the human brain for the same peak overpressures.

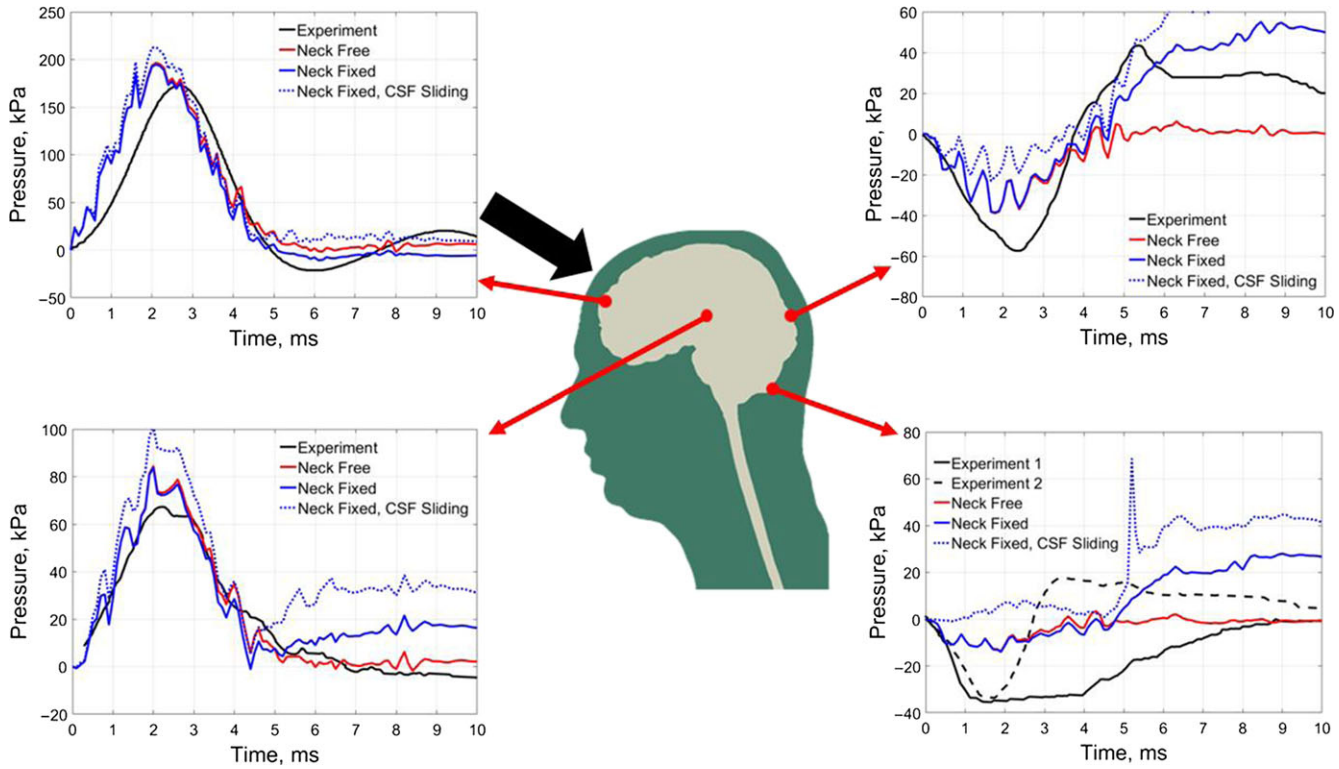

FIGURE 3. Experimental setup and results of Nahum et al.[31] Large arrow shows the direction of impact on the cadaver head.

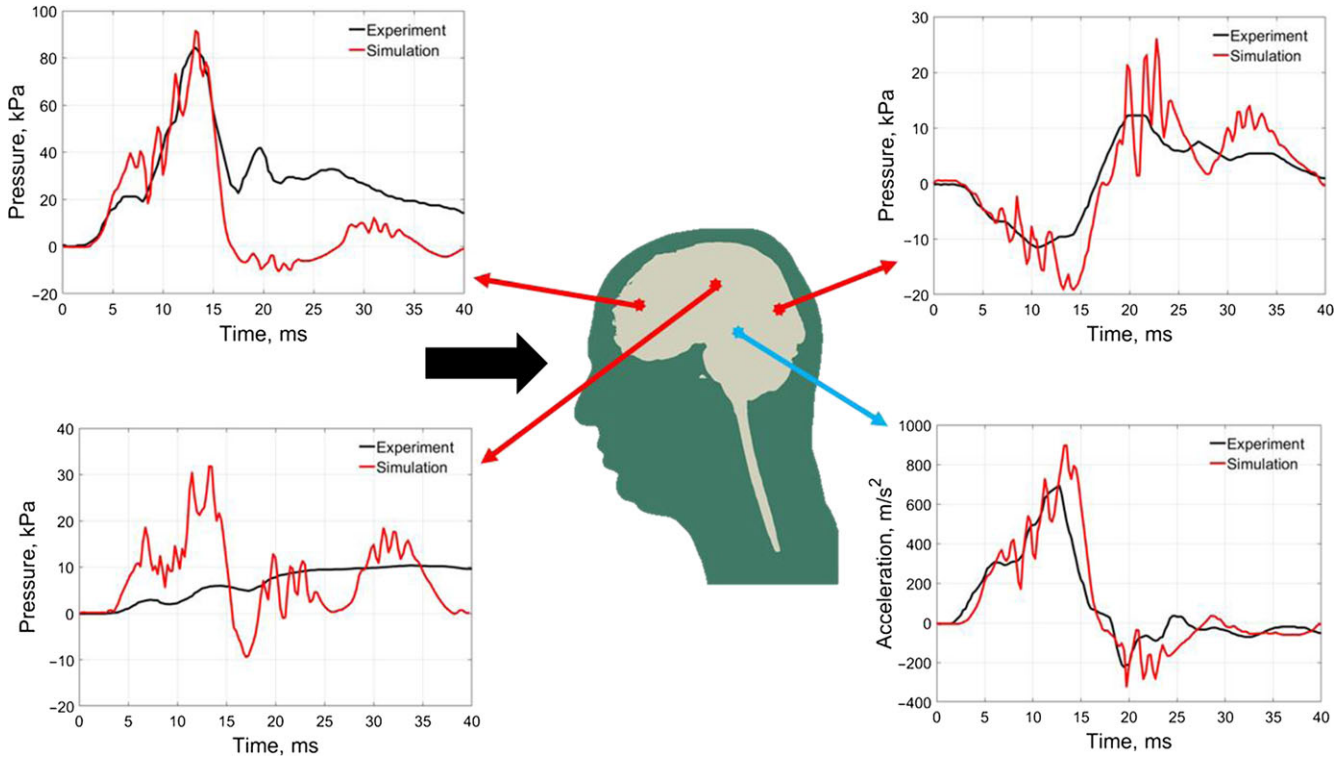

FIGURE 4. Experimental setup and results of Trosseille et al.[32] Large arrow shows the direction of impact on the cadaver head.

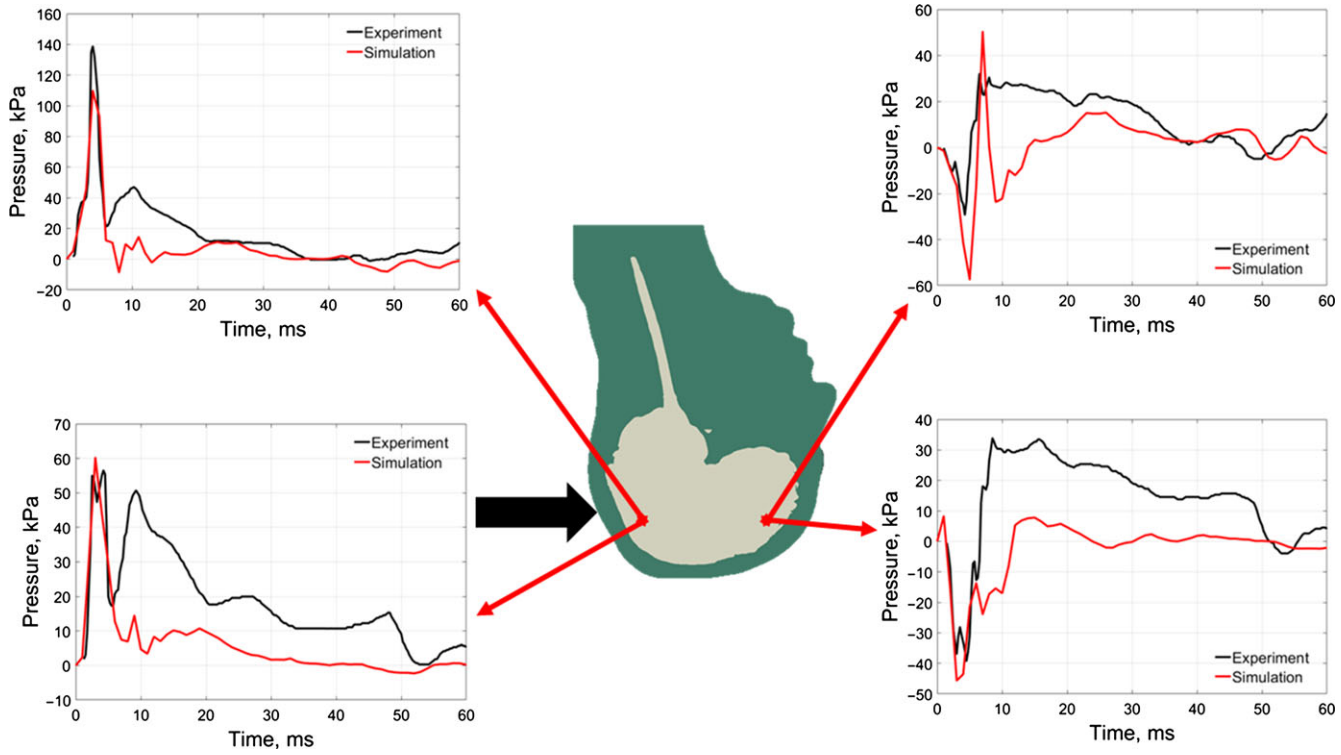

FIGURE 5. Experimental setup and results of Hardy et al.[33,34] Large arrow shows the direction of impact on the cadaver head.

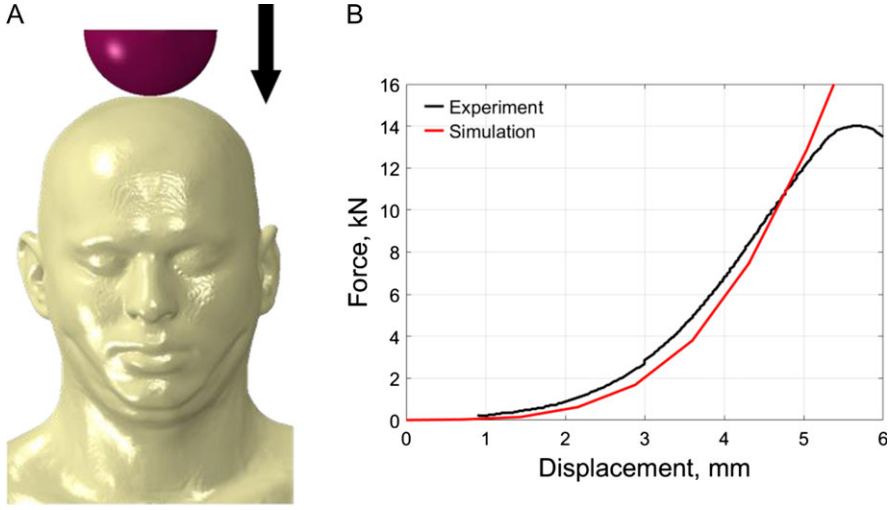

FIGURE 6. (A) Experimental setup and (B) results of Yoganandan et al.[35] Large arrow shows the direction of impact on the cadaver head.

Comparing the pig brain biomechanical response to the human brain response, one can develop a correspondence between the two species using the same injury metrics (or criteria). Based on the results shown, it would be expected that a comparison of the human to the pig to determine equivalent injuries would be best accomplished using a blast with a larger peak overpressure in the pig than in the human. This would allow a direct comparison to be made between the species. In a more complete analysis, multiple injury criteria based on pressures, stresses and strains can be used to develop a comprehensive representation of correspondence rules between the pig and the human brain. Developing such criteria will allow using the experimental data and computational modeling and simulation results for animal subjects to project the injury in humans.

Blast Profile and Orientation Effects

To further examine the effects of a given insult on the predicted injuries, the focus of the effect of blast profile and

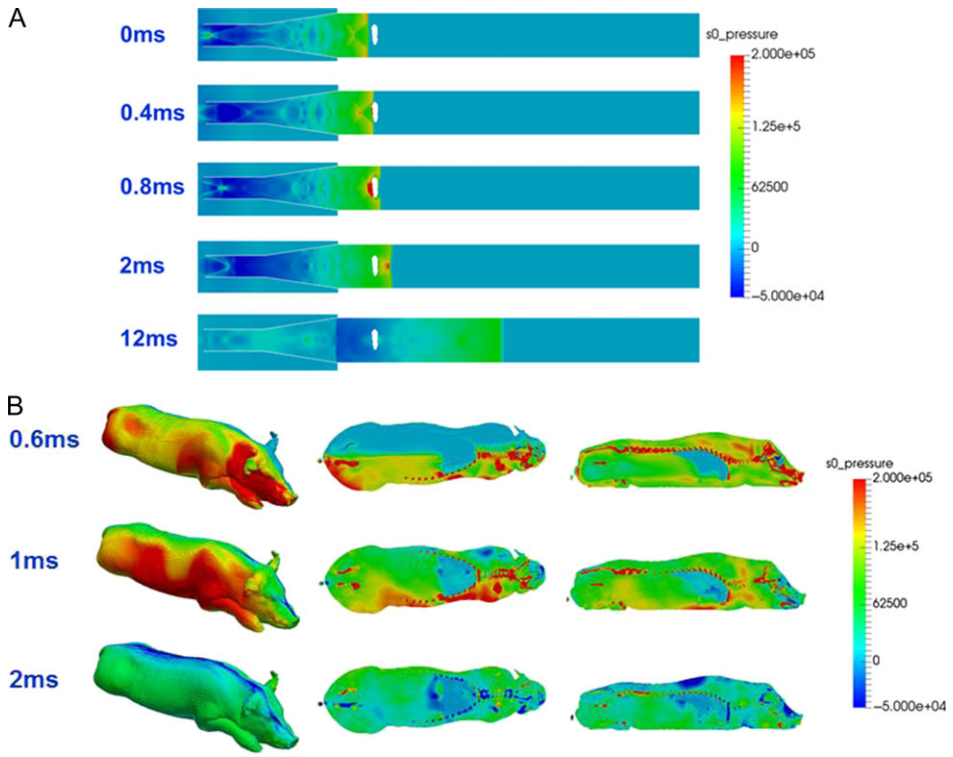

FIGURE 7. Results of CEL analysis with the full pig model using the parameters of Zhu et al.[40] (A) Eulerian analysis results offset by 7.146 ms to account for the time before the wave reaches the pig. (B) Lagrangian analysis results with isometric, transverse, and sagittal views, again offset by 7.146 ms.[41]

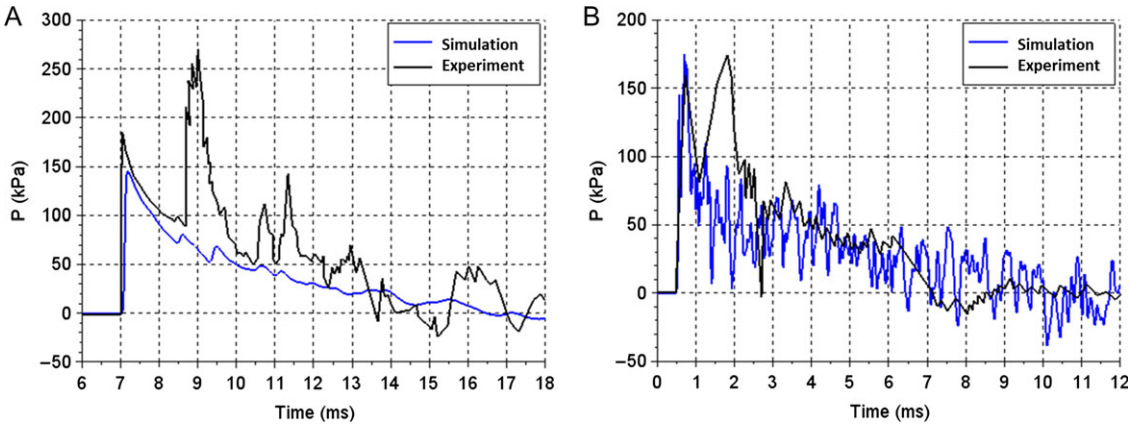

FIGURE 8. Validation results for pressure at (A) the pencil gauge location using Eulerian simulation and (B) the intracranial pressure sensor location using Lagrangian simulation.[41]

orientation effects is limited to the human model only. In this analysis, the human model response is analyzed for both the blast profile effects and the blast impact directionality (i.e., obliquity) effects. The analysis is conducted by applying blast overpressure effects from the front and from the side using idealized Friedlander waves parameterized by peak pressure and positive phase duration. Three peak pressures of 276, 414, and 552 kPa, each with three positive phase durations of 2, 4, and 6 ms, are used for this comparative analysis for both the frontal and side-on orientation. The input pressure profiles and the results based on multiple biomechanical injury criteria and the volume of injured brain as the measure of injury are shown in Figure 13.

Use of pressure-based injury criterion shows a sharp rise that corresponds almost exactly with the time of the peak input pressure plus a delay for the pressure to transduct into the brain. The peak overpressure has the strongest effect on the predicted injury level. The volume of the injured brain vs time in Figure 13B shows three distinct groupings, which correspond to the three peak overpressure inputs. The

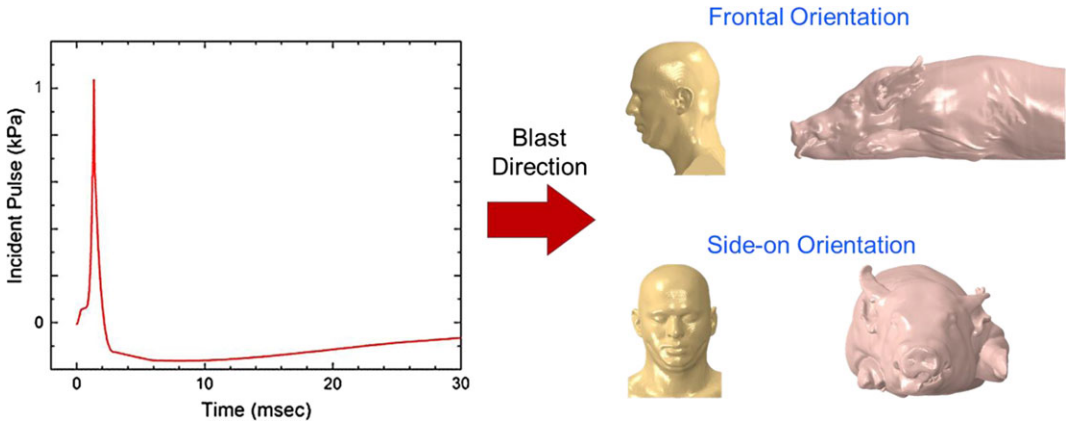

FIGURE 9. Interspecies correspondence study setup. The incident pulse profile is normalized by the maximum value and then scaled to the desired maximum for the study.

positive phase duration variation demonstrates that in general a lower positive phase duration, i.e., a lower impulse, shows a reduced volume of injury for the same pressure, thus suggesting that impulse may contribute to the extent of brain injury. It is also noted that as the peak pressure is increased the effect of positive phase duration seems to decrease, as indicated in Figure 13B. Analysis of the effects of blast orientation shows that at higher peak input pressures, injury is more severe in the side-on case but at lower inputs, the frontal case is more severe, as indicated in Figures 13. Lastly, contrary to expectation, equivalent impulses generated from two different pressure-positive phase duration combinations do not correspond to equivalent injuries. This can be seen by comparing the 276 kPa, 4 ms results with the 552 kPa, 2 ms results, both having an impulse of 1,104 kPa ms but differ by approximately 60% injured brain volume. The complex relationship between peak overpressure, duration, and impulse in blast will need to be further analyzed to determine if there are scenarios in which equivalent impulses lead to equivalent injury.

Use of Tresca stress as the injury criterion, Figure 13C, shows the same quick initial response as the pressure criteria. However, the volume of brain injured using the Tresca criteria is substantially lower than that using the pressure criteria, and the peak values are reached much later, in some cases beyond 10 ms. The injured volume time history is attributed to shear wave reflections within the head.

Use of principal strain as the injury criterion, Figure 13D, shows the most interesting results as it is affected by the rate-dependence in the constitutive model. The initial rise in volume percentage of brain injured starts at the same time as pressure-based and Tresca stress-based criteria, but with a much more gradual increase. Further analysis of the volume of the injured brain with respect to time for this criterion is in progress and will be presented in a future paper. Peak incident pressure seems to be the dominant factor in maximum injured volume with positive phase duration being a secondary factor. Regarding the effect of blast orientation, no clear effect of blast orientation is seen based on the current simulation results. Further analysis is needed and will be reported in a future paper.

CONCLUSIONS AND FUTURE WORK

This paper presents the initial framework for developing a correspondence rule between two species based on injury criteria, and provides initial results from a comparative analysis of two validated computational models – one a porcine head model and another a human head-neck model. The simulation models are based on MRI and CT of a Yucatan pig and a 50 percentile, 26-year-old Caucasian male, and validated based on available experimental data. These validated models are then applied to obtain simulation results for multiple peak blast pressures and pressure-time impulses (by varying the positive phase durations) and blast orientations with respect to the head. The biomechanical responses are quantified based on volume percentage of brain affected with respect to pressure profiles and blast orientation. The analysis utilized injury criteria based on threshold pressure, shear stress and strains from the literature. The initial results show the feasibility of correspondence rules using injury criteria between species, although the injury criterion chosen appears to influence the correspondence rules. Ongoing research is directed at quantifying the effects of blast peak overpressure and positive phase duration and subject orientation on injured brain volume, with a view to developing the correspondence rules between species. However, based on the current results, it can be generally said that a higher peak overpressure and positive phase duration causes a higher injured volume, a frontal impact shows lower injury than a side-on impact at high peak overpressures but the reverse is true at lower peak pressures, and the pig fairs better than a human for a given blast. Further work will be directed at validating the models against high rate blast data, once that data becomes more readily available.

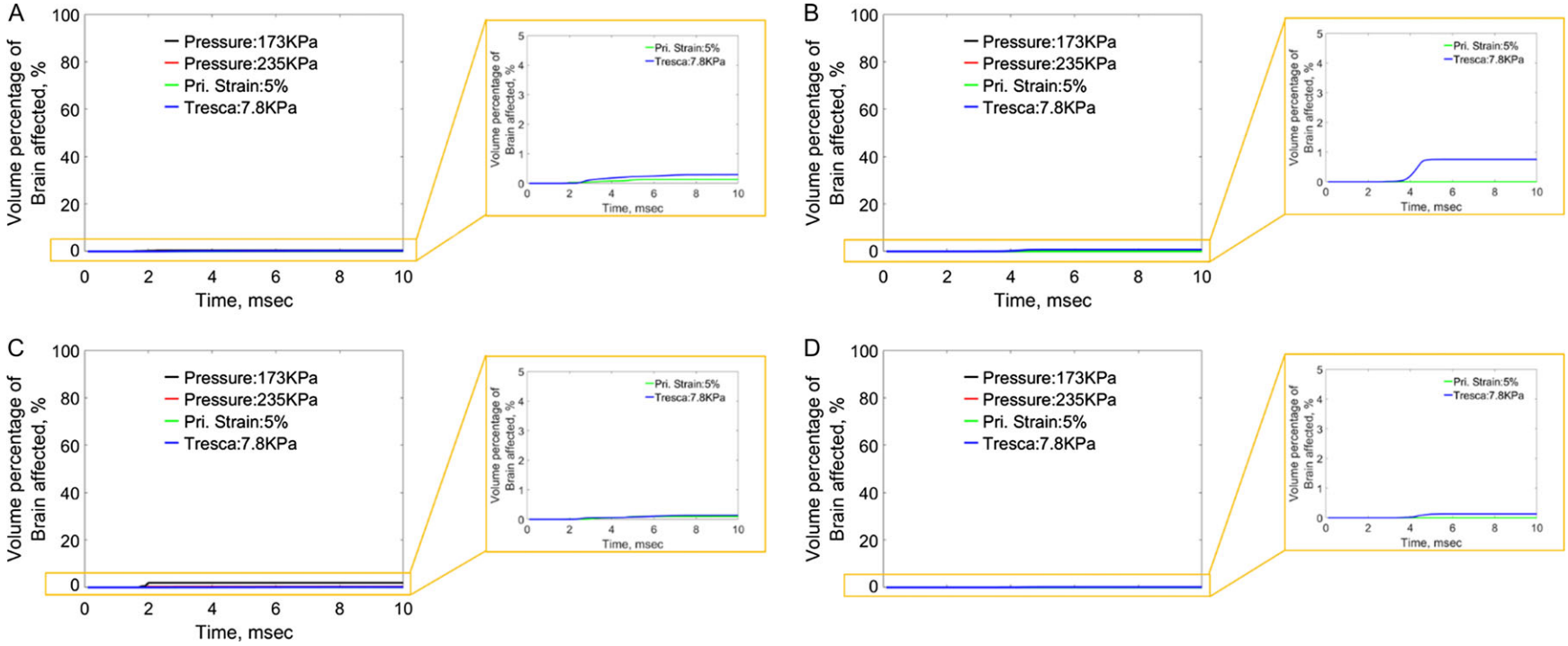

FIGURE 10. Interspecies correspondence study predicted injury results at a 37 psi (255 kPa) peak pressure. (A) human frontal orientation, (B) pig frontal orientation, (C) human side-on orientation, and (D) pig side-on orientation.

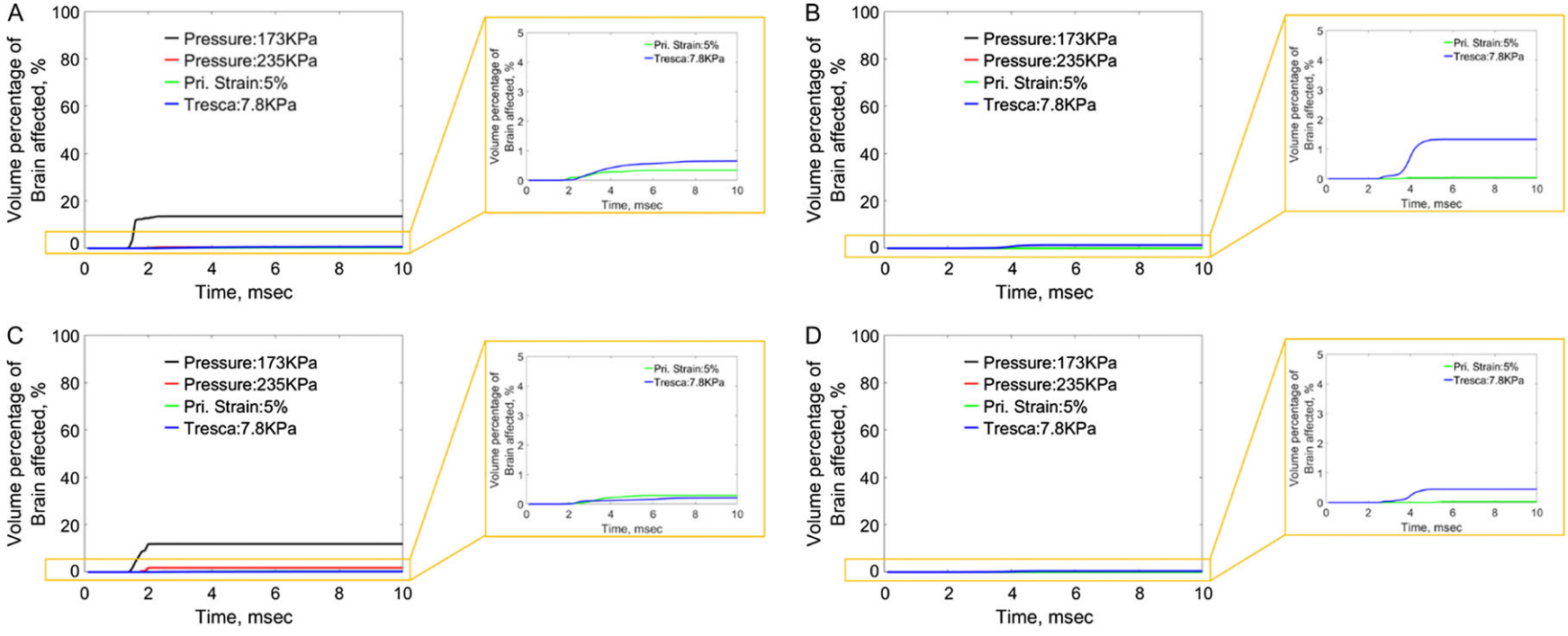

FIGURE 11. Interspecies correspondence study predicted injury results at a 50 psi (345 kPa) peak pressure. (A) human frontal orientation, (B) pig frontal orientation, (C) human side-on orientation, and (D) pig side-on orientation.

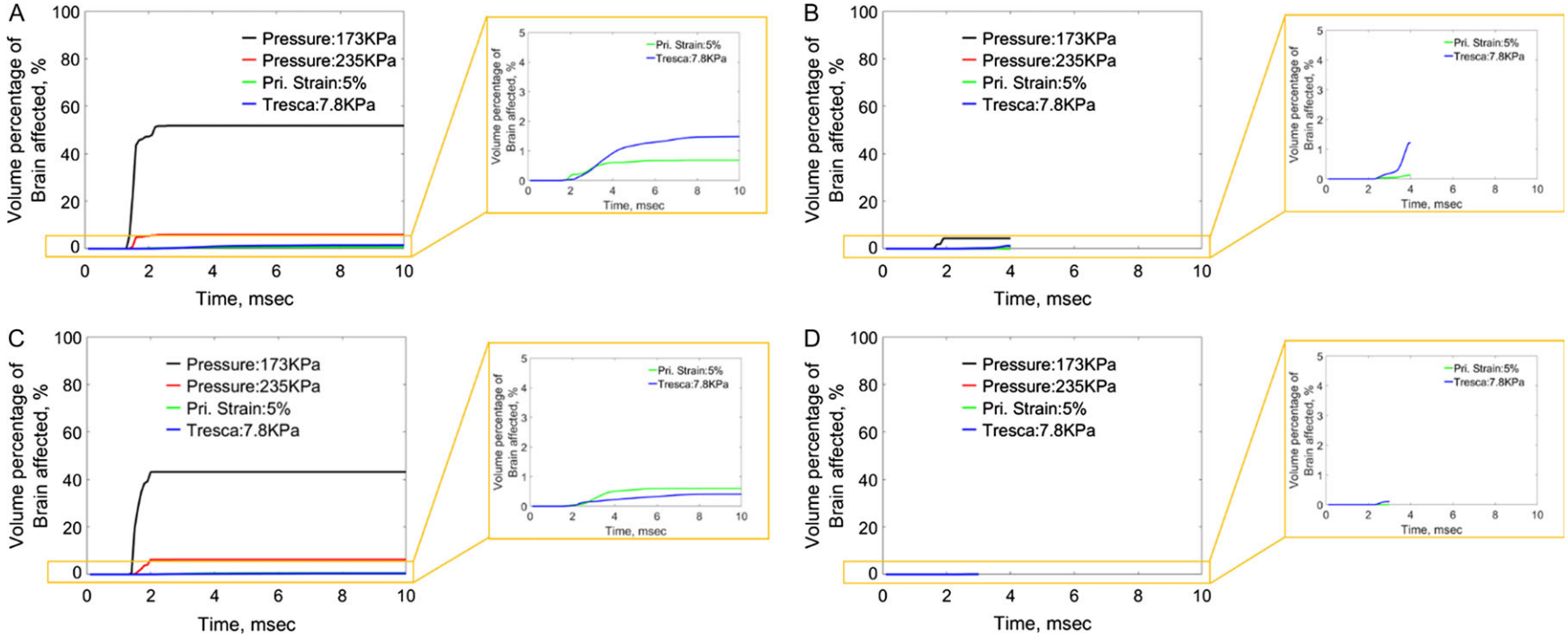

FIGURE 12. Interspecies correspondence study predicted injury results at a 62 psi (427 kPa) peak pressure. (A) human frontal orientation, (B) pig frontal orientation, (C) human side-on orientation, and (D) pig side-on orientation.

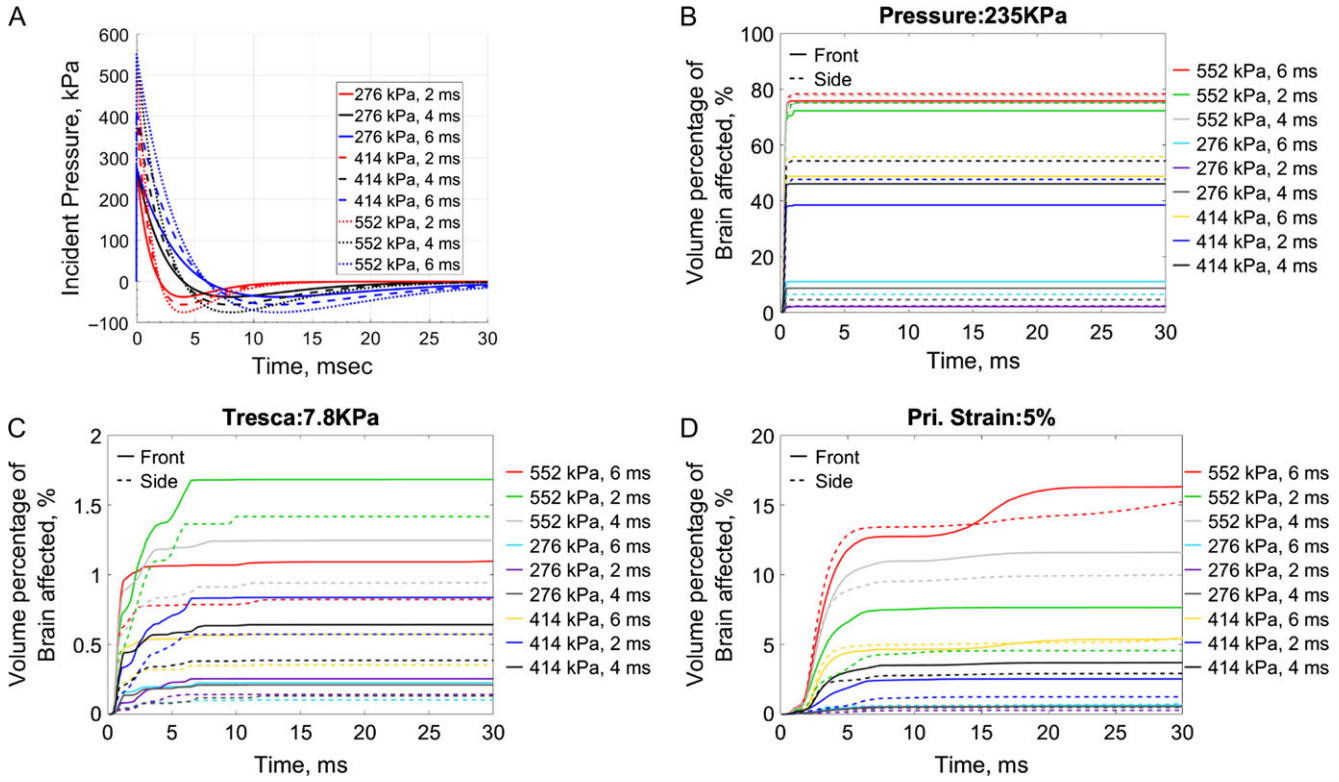

FIGURE 13. Friedlander wave inputs to the human model simulation to determine blast and orientation effects and the resulting predicted injury using (A) 235 kPa pressure criteria, (B) 7.8 kPa Tresca stress criteria, and (C) 5% principal strain criteria.

PREVIOUS PRESENTATION

Presented as a poster at the 2017 Military Health System Research Symposium, August 2017, Kissimmee, FL; abstract # MHSRS-17–1650.

FUNDING

This work was supported by the Office of Naval Research (ONR) under contract number N001415WX00531 and the Department of Defense (DoD) High Performance Computing Modernization Program (HPCMP) using the Air Force Research Laboratory (AFRL) Major Shared Resource Center (MSRC) under project 416, subproject 231. This supplement was sponsored by the Office of the Secretary of Defense for Health Affairs.

ACKNOWLEDGMENTS

The authors acknowledge Dr Ross Cotton from Simpleware for the generation of the finite element meshes, and Dr Siddiq Qidwai from National Science Foundation (formerly at NRL) and Dr Thomas O'Shaughnessy from NRL for technical discussions. The authors also acknowledge Dr Tim Bentley from ONR for his support and technical discussions. This material is declared a work of the U.S. Government and is not subject to copyright protection in the United States. Approved for public release; distribution is unlimited.

REFERENCES

1. Elsayed NM, Gorbunov NV: Chapter 8: biochemical mechanism(s) of primary blast injury: the role of free radicals and oxidative stress. In: Elsayed and Atkins' Explosion and Blast Related Injuries. Oxford, UK, Elsevier Academic Press, 2008.
2. Hrapko M, Van Dommelen JA, Peters GW, Wismans JS: The influence of test conditions on characterization of the mechanical properties of brain tissue. J Biomech Eng 2008; 130(3): 031003.
3. Povlishock JT, Hayes RL, Michel ME, McIntosh TK: Workshop on animal models of traumatic brain injury. J Neurotrauma 1994; 11(6): 723–32.
4. Cenci MA, Whishaw IQ, Schallert T: Animal models of neurological deficits: how relevant is the rat? Nat Rev Neurosci 2002; 3(7): 574–9.
5. Sereno MI, Tootell RB: From monkeys to humans: what do we now know about brain homologies? Curr Opin Neurobiol 2005; 15(2): 135–44.
6. Willinger R, Kang HS, Diaw B: Three-dimensional human head finite-element model validation against two experimental impacts. Ann Biomed Eng 1999; 27(3): 403–10.
7. Kleiven S, von Holst H: Consequences of head size following trauma to the human head. J Biomech 2002; 35(2): 153–60.
8. Horgan TJ, Gilchrist MD: The creation of three-dimensional finite element models for simulating head impact biomechanics. Int J Crashworthines 2003; 8(4): 353–66.
9. Takhounts EG, Ridella SA, Hasija V, et al: Investigation of traumatic brain injuries using the next generation of simulated injury monitor (SIMon) finite element head model. Stapp Car Crash J 2008; 52: 1.
10. Zhang L, Yang KH, King AI: A proposed injury threshold for mild traumatic brain injury. Transactions-American Society of Mechanical Engineers. J Biomech Eng 2004; 126(2): 226–36.
11. Mao H, Zhang L, Jiang B, et al: Development of a finite element human head model partially validated with thirty five experimental cases. J Biomech Eng 2013; 135(11): 111002.
12. Moore DF, Jérusalem A, Nyein M, Noels L, Jaffee M, Radovitzky R.: Computational biology – modeling of primary blast effects on the central nervous system. Neuroimage 2009; 47: T10–20.
13. Taylor PA, Ford CC: Simulation of blast-induced early-time intracranial wave physics leading to traumatic brain injury. J Biomech Eng 2009; 131(6): 061007.

14. NASA: Volume 1, Section 3: Anthropometry and Biomechanics. Man-System Integration Standards, NASA; 1995. Available at https://msis.jsc.nasa.gov/sections/section03.htm; accessed May 28, 2018.
15. Young PG, Beresford-West TB, Coward SR, Notarberardino B, Walker B, Abdul-Aziz A: An efficient approach to converting three-dimensional image data into highly accurate computational models. Philos Trans R Soc Lond A 2008; 366(1878): 3155–73.
16. Cotton RT, Pearce CW, Young PG, et al: Development of a geometrically accurate and adaptable finite element head model for impact simulation: the Naval Research Laboratory – Simpleware Head Model. Comput Methods Biomech Biomed Engin 2016; 19(1): 101–13.
17. Young P, Tabor G, Collins T, Richterova J, Dejuniat E, Beresford-West T: Automating the generation of 3D finite element models based on medical imaging data. SAE Technical Paper 2006-07-04. Available at https://www.sae.org/publications/technical-papers/content/2006-01-0231/; accessed May 28, 2018.
18. Thibault KL, Margulies SS: Age-dependent material properties of the porcine cerebrum: effect on pediatric inertial head injury criteria. J Biomech 1998; 31(12): 1119–26.
19. Brewick P, Saunders R, Bagchi A: Biomechanical modeling of the human head. DTIC 2017. Available at http://www.dtic.mil/dtic/tr/fulltext/u2/1040988.pdf; accessed May 28, 2018.
20. Kruse SA, Rose GH, Glaser KJ, et al: Magnetic resonance elastography of the brain. Neuroimage 2008; 39(1): 231–7.
21. Tan XG, Przekwas AJ: A computational model for articulated human body dynamics. Int J Hum Fact Model Simul 2011; 2(1–2): 85–110.
22. Tan XG, Przekwas AJ, Gupta RK: Computational modeling of blast wave interaction with a human body and assessment of traumatic brain injury. Shock Waves 2017; 27(6): 889–904.
23. Takhounts EG, Eppinger RH, Campbell JQ, Tannous RE: On the development of the SIMon finite element head model. Stapp Car Crash J 2003; 47: 107.
24. Kang HS, Willinger R, Diaw BM, Chinn B: Validation of a 3D anatomic human head model and replication of head impact in motorcycle accident by finite element modeling. SAE Technical Paper 1997-11-12. Available at https://www.sae.org/publications/technical-papers/content/973339/; accessed May 28, 2018.
25. Deck C, Willinger R: Improved head injury criteria based on head FE model. Int J Crashworthines 2008; 13(6): 667–78.
26. Margulies SS, Thibault LE: A proposed tolerance criterion for diffuse axonal injury in man. J Biomech 1992; 25(8): 917–23.
27. Wright RM, Ramesh KT: An axonal strain injury criterion for traumatic brain injury. Biomech Model Mechanobiol 2012; 11(1–2): 245.
28. Kleiven S: Predictors for traumatic brain injuries evaluated through accident reconstructions. Stapp Car Crash J 2007; 51: 81.
29. Anderson AE, Ellis BJ, Weiss JA: Verification, validation and sensitivity studies in computational biomechanics. Comput Methods Biomech Biomed Engin 2007; 10(3): 171–84.
30. Henninger HB, Reese SP, Anderson AE, Weiss JA: Validation of computational models in biomechanics. Proc Inst Mech Eng H 2010; 224(7): 801–12.
31. Nahum AM, Smith R, Ward CC: Intracranial pressure dynamics during head impact. SAE Technical Paper 1977-02-01. Available at https://www.sae.org/publications/technical-papers/content/770922/; accessed May 28, 2018.
32. Trosseille X, Tarriere C, Lavaste F, Guillon F, Domont A: Development of a FEM of the human head according to a specific test protocol. SAE Technical Paper 1992-11-01. Available at https://www.sae.org/publications/technical-papers/content/922527/; accessed May 28, 2018.
33. Hardy WN, Foster CD, Mason MJ, Yang KH, King AI, Tashman S: Investigation of head injury mechanisms using neutral density technology and high-speed biplanar X-ray. Stapp Car Crash. Journal 2001; 45: 337–68.
34. Hardy WN, Mason MJ, Foster CD, et al: A study of the response of the human cadaver head to impact. Stapp Car Crash. Journal 2007; 51: 17.
35. Yoganandan N, Pintar FA, Sances AN Jr, et al: Biomechanics of skull fracture. J Neurotrauma 1995; 12(4): 659–68.
36. Prange MT, Margulies SS: Regional, directional, and age-dependent properties of the brain undergoing large deformation. J Biomech Eng 2002; 124(2): 244–52.
37. Gur RC, Mozley PD, Resnick SM, et al: Gender differences in age effect on brain atrophy measured by magnetic resonance imaging. Proc Natl Acad Sci USA 1991; 88(7): 2845–9.
38. Gefen A, Gefen N, Zhu Q, Raghupathi R, Margulies SS: Age-dependent changes in material properties of the brain and braincase of the rat. J Neurotrauma 2003; 20(11): 1163–77.
39. Deck C, Willinger R: The current state of the human head finite element modelling. Int J Veh Saf 2009; 4(2): 85–112.
40. Zhu F, Skelton P, Chou CC, Mao H, Yang KH, King AI: Biomechanical responses of a pig head under blast loading: a computational simulation. Int J Numer Method Biomed Eng 2013; 29(3): 392–407.
41. Tan XG, Saunders RN, Bagchi A: Validation of a full porcine finite element model for blast induced TBI using a coupled Eulerian-Lagrangian approach. In Proceeding of the ASME 2017 International Mechanical Engineering Congress & Exposition, Tampa, FL. Available at http://proceedings.asmedigitalcollection.asme.org/proceeding.aspx?articleid=2668862&resultClick=3; accessed May 28, 2018.